J Mater Sci (2010) 45:1459–1463
DOI 10.1007/s10853-009-4101-8

One-step thermal synthesis of binary manganese iron cyclotetraphosphate $MnFeP_4O_{12}$

Banjong Boonchom · Naratip Vittayakorn

Received: 3 August 2009 / Accepted: 30 November 2009 / Published online: 11 December 2009

Abstract The manganese iron cyclotetraphosphate ($MnFeP_4O_{12}$) was synthesized through one-step thermal synthesis at 700 °C using the mixing of manganese and iron metals and phosphoric acid in the presence of water–acetone media. Both FTIR and XRD results indicate the cyclotetraphosphate ($P_4O_{12}^{4-}$) structure and a pure monoclinic phase with space group *C2/c* ($Z = 4$). The morphology and crystallite size for the $MnFeP_4O_{12}$ obtained from SEM data and X-ray line broadening show non-uniform particles and 30 ± 9 nm, respectively. The magnetic study of the synthesized $MnFeP_4O_{12}$ shows superparamagnetic behavior, which is important for specific application. Some physical properties of the synthesized $MnFeP_4O_{12}$ powder presented for the first time are comparable with those from individual $M_2P_4O_{12}$ (M = Mn and Fe) and a binary metal compound as $CoFeP_4O_{12}$.

Introduction

The metal(II) phosphates have considerable industrial interesting properties such as ceramics, catalysts, fluorescent materials, dielectrics, metal surface treatment agents, detergents, food additives, fuel cell materials, pigment, etc. [1–4]. Metal cyclotetraphosphates $M_2P_4O_{12}$ and binary metal cyclotetraphosphates $M_{2-x}A_xP_4O_{12}$ (M and A = Mg, Ca, Mn, Co, Ni, Zn, or Cu; $0 < x < 2$), are isostructural, were examined for potential applications as special inorganic pigments [5, 6]. All these compounds have similar X-ray diffraction patterns and close unit cell parameters, which crystallize in monoclinic space group *C2/c* (Z = 4) [7]. They were first described by Trojan et al. [6, 8, 9] and prepared by mixing starting materials, followed by calcination, crushing, and adjusting their color [9–11]. Many methods have been employed to synthesize single or binary metal cyclotetraphosphate, including two-step thermal method [6, 8, 9], hydrothermal synthesis [5], and the condensation of binary metal(II) dihydrogenphosphate hydrates ($M_{1-y}A_y(H_2PO_4)_2{\cdot}nH_2O$ where $0 < y < 1$; $1 < n < 4$) [12, 13]. In our previous work, the $MnFeP_4O_{12}$ prepared by the calcinations of $Mn_{0.5}Fe_{0.5}(H_2PO_4)_2{\cdot}nH_2O$ at 500 °C uses several processes [12]. These previously reported methods were long time consuming (>5 h) with high temperature (800–1000 °C) and were the evolved toxic gases (NO_2 and CO_2). These works are of interest because it appears economically advantageous and environmentally friendly to substitute a portion of the divalent metal with a less costly divalent element, which influences many properties, for example, the color of pigments, thermally and chemically stable compounds [6, 8], anticorrosion ability, and luminescence [8, 9, 14, 15]. However, it is relevant to synthesize binary cyclotetraphosphate and its solid solution because changing the metal ratio influences its useful properties.

Herein, we report for the first time the synthesis of a binary manganese iron cyclotetraphosphate, $MnFeP_4O_{12}$ by one-step thermal synthesis using solid state route of manganese and iron metals and phosphoric acid in water–acetone medium. This method is a simple, rapid, cost-effective, and environmental friendly route for synthesis of

---

B. Boonchom (✉)
King Mongkut's Institute of Technology Ladkrabang,
Chumphon Campus, 17/1 M. 6 Pha Thiew District, Chumphon
86160, Thailand
e-mail: kbbanjon@kmitl.ac.th

B. Boonchom · N. Vittayakorn
Advanced Materials Science Research Unit, Department
of Chemistry, Faculty of Science, King Mongkut's Institute
of Technology Ladkrabang, Bangkok 10520, Thailand

$MnFeP_4O_{12}$, exhibiting the differences of some physical and chemical properties from those in our previously report [12, 16, 17]. The synthesized sample was characterized by X-ray powder diffraction (XRD), Fourier transform infrared (FTIR), scanning electron microscope (SEM), and a vibrating sample magnetometer (VSM) techniques.

Experimental

Reagent and apparatus

The starting reagents are Mn, Fe, H_3PO_4, and acetone. All chemicals were of p.a. quality (Merck). As metal sources we use crystalline Mn and Fe metals since they display: (i) a moderate stability at storage (with respect to bond oxidation to Fe(II) and Mn(II) and dehydration, which ensures an exact stoichiometry in the final product; (ii) appearance of reducing gaseous products (H_2, H_2O, CO, or CO_2) during the calcination process. The manganese and iron contents of $MnFeP_4O_{12}$ were determined by dissolving in 0.0126 M hydrochloric acid using atomic absorption spectrophotometry (AAS, Perkin Elmer, Analyst100). The phosphorus content was determined by colorimetric analysis. The room temperature FTIR spectrum was recorded in the range of 4000–370 cm^{-1} with 8 scans on a Perkin-Elmer Spectrum GX FT-IR/FT-Raman spectrometer with the resolution of 4 cm^{-1} using KBr pellets (KBr, spectroscopy grade, Merck). The structure and crystallite size of the product were studied by X-ray powder diffraction using a X-ray diffractometer (Phillips PW3040, The Netherlands) with Cu Kα radiation ($\lambda = 0.15406$ nm). The Scherrer method was used to evaluate the crystallite size [18]. The morphology of the product was examined with scanning electron microscope using LEO SEM VP1450 after gold coating. The magnetic study of the product was examined at room temperature (20 °C) using a vibrating sample magnetometer (VSM 7403, Lake Shore, USA).

Preparation of manganese iron cyclotetraphosphate $MnFeP_4O_{12}$

Typical procedure, 0.5494 g of Mn (c), 0.5584 g of Fe (c), and 10 mL acetone were put in a beaker with mechanical stirring. The mixture was added by 5 mL of 70% H_3PO_4 (86.4% w/w H_3PO_4 dissolved in DI water) with continuous stirring at ambient temperature (10 min). The reactant mixture was transferred to a crucible, which was heated in the furnace at 700 °C for 2 h in an air atmosphere. The obtained pale gray powder was crushed and washed repeatedly with water until no PO_4^{3-} was detected in filtrate. Then, the powder was washed again for several times with methanol and dried at room temperature. The reaction equation can be expressed as:

$$\begin{aligned} &Mn(s) + Fe(s) + 4H_3PO_4(aq) \\ &\xrightarrow{\text{Acetone, } 700\,^{\circ}\text{C in air atmosphere}} MnFeP_4O_{12}(s) + 4H_2O(g) \\ &\quad + 2H_2(g) \end{aligned} \tag{1}$$

Results and discussion

Chemical analysis of $MnFeP_4O_{12}$

The chemical compositions of the synthesized $MnFeP_4O_{12}$ were analyzed according to the discussed methods. The data showed that manganese, iron, and phosphorus mass percentages were 14.55, 14.30, and 31.92 wt%, respectively. In other words, mole ratio of Mn:Fe:P in the synthetic product is equal to 1.03:1.00:4.02. This indicates that the general formula would be $MnFeP_4O_{12}$.

XRD analysis of $MnFeP_4O_{12}$

Figure 1 shows the XRD pattern of the product $MnFeP_4O_{12}$ obtained at 700 °C. The higher intensities of XRD peaks observed indicate crystallization as well as particle sizes of the product. On the basis of isostructural, XRD patterns of the individual $M_2P_4O_{12}$ (when M = Mn and Fe) and the binary $M_{1-x}A_xP_4O_{12}$ are quite similar due to the electric charges of cations are equivalent, and the radii of cations are close to each other. Consequently, we can draw a conclusion that the synthesized $MnFeP_4O_{12}$ is solid solution and not a mixture of the individual ones. All the detectable peaks in the figure are found to be in agreement with monoclinic phase, space group *C2/c* ($Z = 4$) from PDF card 380314 for $Mn_2P_4O_{12}$ and PDF card 782285 for

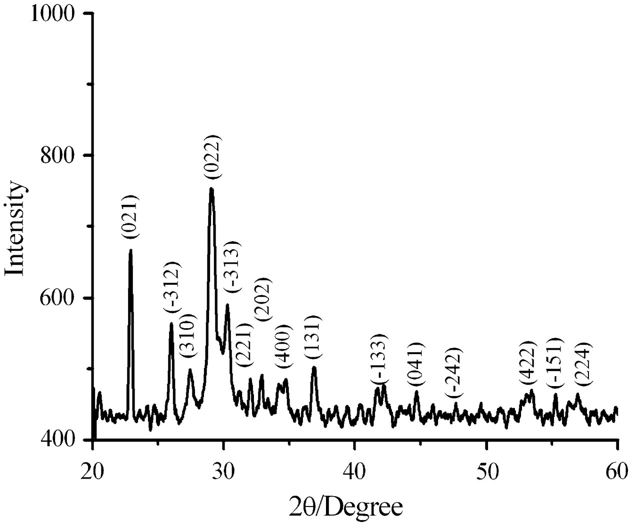

Fig. 1 XRD pattern of $MnFeP_4O_{12}$

Table 1 Average particle size and lattice parameters of $MnFeP_4O_{12}$ calculated from XRD data

Compounds	Systems	*a* (Å)	*b* (Å)	*c* (Å)	*β* (°)	Average crystallite size (nm)
$Mn_2P_4O_{12}$	PDF no 380314	11.88	8.588	10.137	119.21	–
	Ref. [16]	11.784(0)	8.913(4)	10.055(6)	119.95(3)	29 ± 9
$MnFeP_4O_{12}$	This work	12.02(0)	8.23(0)	10.57(0)	118.89(2)	30 ± 9
	Ref. [12]	12.02(8)	8.42(2)	10.10(4)	119.11(5)	69 ± 21
$Fe_2P_4O_{12}$	PDF no.782285	11.94	8.37	9.93	118.74	
	Ref. [17]	12.80(0)	8.80(4)	10.56(0)	118.67(4)	29 ± 6

$Fe_2P_4O_{12}$ and the XRD pattern of the prepared sample is in agreement with that of $MnFeP_4O_{12}$, obtained by the thermal transformation of $Mn_{0.5}Fe_{0.5}(H_2PO_4)_2 \cdot nH_2O$ at 500 °C. According to the Scherrer formula: $D = 0.89\lambda/\beta\cos\theta)$, where D is crystallite diameter, $\lambda = 0.15406$ nm (the wavelength of X-ray radiation), θ is the diffraction angle, and β is the full width at half maximum (FWHM) [18]. The crystallite size of the product are estimated from the strong peaks below 40° fro 2θ. The resulting crystallite size of the product is 30 ± 9 nm. The lattice parameters determined from the XRD spectra are very close to the standard data file (from PDF no. 380314 for $Mn_2P_4O_{12}$ and PDF no. 782285 for $Fe_2P_4O_{12}$) and $MnFeP_4O_{12}$ reported in the literature (Table 1) [12, 16, 17].

FT-IR spectroscopic analysis of $MnFeP_4O_{12}$

The FTIR spectrum of the product $MnFeP_4O_{12}$ is seen in Fig. 2. The crystal structure is a three-dimensional framework of MO_6 (M = Mn or Fe) polyhedral linked with P_4O_{12} rings by M–O–P. The vibrational modes of $P_4O_{12}{}^{4-}$ ion observed in the frequency range of 370–1400 cm^{-1} are assigned according to the literature [16, 17, 19]. The strong band at 1226 cm^{-1} is due to the asymmetric stretching frequency of the $PO_2{}^{2-}$ radical, while the bands at 1100–100 cm^{-1} to the symmetric stretching frequencies of the $PO_2{}^{2-}$ radical. The bending modes are expected in the area 600–400 cm^{-1} ($PO_2{}^{2-}$ radical) and 400–370 cm^{-1} (P–O–P bridge). The metal–O stretching usually appears in the bending mode region as the bending modes of the P–O–P bridge and absorption bands associated with these vibrations are usually very weak. One strong band at 970 cm^{-1} is assigned to the asymmetric of the P–O–P bridge. Three bands between 800 and 700 cm^{-1} are due to symmetric stretching frequencies of the P–O–P bridge. The observation of a strong ν_sPOP band is known to be the most striking feature of cyclotetraphosphate spectra, along with the presence of the $\nu_{as}OPO^-$ band, which indicate the cyclic structure of the $[P_4O_{12}]^{4-}$ anion. This FTIR result is consistent with X-ray diffraction data [5].

SEM analysis of $MnFeP_4O_{12}$

Figure 3 shows the SEM micrograph of $MnFeP_4O_{12}$ product. The whole thermal transformation phase changed

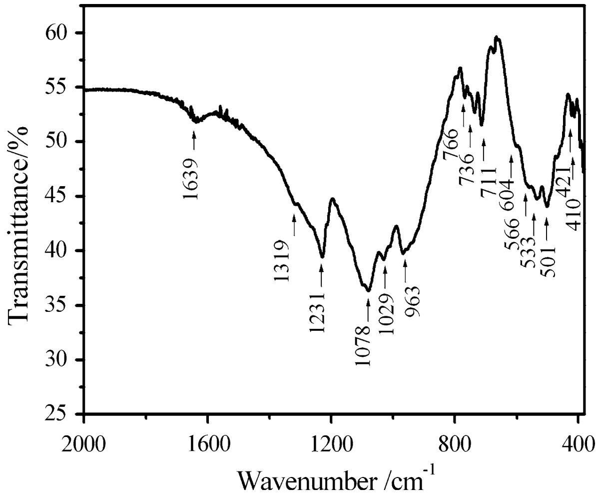

Fig. 2 FTIR spectrum of $MnFeP_4O_{12}$

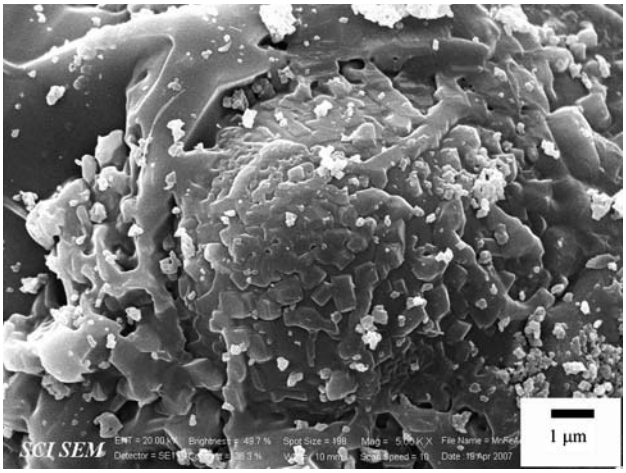

Fig. 3 SEM micrograph of $MnFeP_4O_{12}$

particle shape and size of the product composed of a high agglomerate of non-uniform particles, which is not similar to those of $M_2P_4O_{12}$ (M = Mn or Fe) (Fig. 3) and $MnFeP_4O_{12}$ obtained by thermal condensation of $Mn_{0.5}Fe_{0.5}(H_2PO_4)_2\cdot nH_2O$ in our previous studies [12, 16, 17] The highly agglomerate of $MnFeP_4O_{12}$ powder is possibly caused by the process of the decomposition process in acetone medium. There is strong agglomeration phenomenon among the particles of $MnFeP_4O_{12}$, which is attributed that the each other absorption exists among particles with the layered structure compound. The SEM result indicates that the grain sizes of $MnFeP_4O_{12}$ are not consistent with the crystallite sizes in the XRD analysis because the exact particle nucleation and growth mechanisms are caused.

VSM magnetometer

Magnetization curve (M–H loop) for $MnFeP_4O_{12}$ powder obtained from room temperature VSM measurement is illustrated in Fig. 4. Magnetization did not reach saturation, even at maximum applied magnetic field in range of ±10,000 Oe, and no hysteresis was found, which indicated that the studied product is superparamagnetic [20]. Specific saturated magnetization (M_s) value (14.09 emu/g) for the studied $MnFeP_4O_{12}$ powder [12] is close to that of $CoFeP_4O_{12}$ (14.24 emu/g)[15]. But the superparamagnetic property for the studied compound is significantly different from the ferromagnetic properties for $Fe_2P_4O_{12}$ (85.01 emu/g) [17] and $MnFeP_4O_{12}$ (13.14 emu/g) [12] (obtained from thermal condensation of $Mn_{0.5}Fe_{0.5}(H_2PO_4)_2\cdot nH_2O$ at 500 °C) and the diamagnetic property for $Mn_2P_4O_{12}$ [16]. Compared with the M_s of Fe_3O_4 bulk (92 emu/g) and Fe_3O_4 nanoparticles (in a range of 30–50 emu/g), the M_s of $MnFeP_4O_{12}$ was lower, which might be attributed the nature of samples; crystal structure, shape, and particle size [21]. If Mn(II) is inserted to $Fe_2P_4O_{12}$, the magnetism would decrease significantly, since the effective metal radius of $MnFeP_4O_{12}$ was different from its core radius of $Fe_2P_4O_{12}$. This result indicates that the different magnetic property of $MnFeP_4O_{12}$ is caused by the presence of Mn ions in substitution position of Fe ions in the skeleton. This study demonstrates that the synthesized $MnFeP_4O_{12}$ is truly superparamagnetic, which is a unique feature of magnetic materials. This material may be used in modern technologies including magnetic resonance imaging contrast agents, data lifetime in high density information storage, ferrofluid technology, and magnetocaloric refrigeration [19–21].

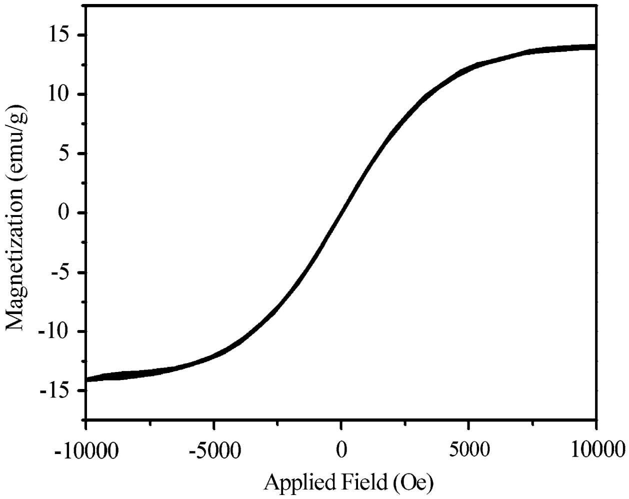

Fig. 4 The specific magnetization of $MnFeP_4O_{12}$ as a function of field, measured at 20 °C

Conclusions

This research has successfully achieved a simple one-step thermal synthesis of a monoclinic binary $MnFeP_4O_{12}$ in the presence of water–acetone media. FTIR, XRD, SEM, and VSM results suggested the formation of a binary manganese iron cyclotetraphosphate $MnFeP_4O_{12}$. The FTIR and XRD data confirmed the most feature of cyclic polyphosphate anion, which indicated the dominant cyclotetraphosphate of $P_4O_{12}{}^{4-}$ anion. The morphology and crystallite size of $MnFeP_4O_{12}$ show a high agglomerate of non-uniform particles and polycrystalline having crystallite size of 30 ± 9 nm, as estimated by SEM and XRD, respectively. The magnetic analysis of the synthesized $MnFeP_4O_{12}$ shows superparamagnetic property, having no hysteresis loop in the range of $-10{,}000\ \mathrm{Oe} < H < 10{,}000\ \mathrm{Oe}$ with the specific magnetization of 14.09 emu/g at 10 kOe. This research displays that the simple, cost-effective, rapid time consumption, and environmental friendly method is necessary for elaboration of technology and academic scientist to produce the cyclotetraphosphate of transition metals, which may be useful for potentially applications as super phosphate and micronutrient fertilizers, inorganic ceramic pigment, catalyst, fuel cell material and corrosion-proof compositions.

Acknowledgements This work is financially supported by the Thailand Research Fund (TRF), the Commission on Higher Education (CHE): Research Grant for New Scholar and the National Nanotechnology Center (NANOTEC) NSTDA, Ministry of Science and Technology, Thailand.

References

1. Hu X, Yan S, Ma L, Wan G, Hu J (2009) Powder Technol 192:27
2. Amri M, Zouari N, Mhiri T, Daoud A, Gravereau P (2006) J Mol Struct 782:16
3. Trojan M, Šulcová P (2000) Dyes Pigments 47:291

4. Boonchom B, Danvirutai C (2008) Ind Eng Chem Res 47:5976
5. Gunsser W, Fruehauf D, Rohwer K, Zimmermann A, Wiedenmann A (1989) J Solid State Chem 82:43
6. Trojan M, Brandová D (1985) Thermochim Acta 88:415
7. Durif A (2005) Solid State Sci 7:760
8. Trojan M, Šulcová P (2000) Thermochim Acta 343:135
9. Trojan M, Šulcová P (2000) J Therm Anal Calorim 60:215
10. Arbi K, Ben Hassen-Chehimi D, Trabelsi-Ayadi M, Silvestre JP (2000) Mater Res Bull 35:1533
11. Naïli H, Ettis H, Mhiri T (2006) J Alloys Compd 424:400
12. Boonchom B, Maensiri S, Youngme S, Danvirutai C (2009) Solid State Sci 11:485
13. Trojan M, Brandová D (1990) Thermochim Acta 161:11
14. Averbuch-Pouchat MT, Durif A (1996) Topics in phosphate Chemistry. World Scienctific, Singapore
15. Boonchom B, Thongkam M, Kongtaweelert S, Vittayakorn N (2009) J Alloys Compd 486:689
16. Boonchom B, Maensiri S, Youngme S, Danvirutai C (2008) Mater Chem Phys 109:404
17. Boonchom B, Maensiri S, Youngme S, Danvirutai C (2008) Ind Eng Chem Res 47:7642
18. Cullity BD (1977) Elements of X-ray diffraction, 2nd edn. Addison-Wesley Publishing, Massachusetts
19. Ramakrishnan V, Aruldhas G (1985) Infrared Phys 25:665
20. Ma H, Qi X-r, Maitani Y, Nagai T (2007) Int J Pharm 333:177
21. Gupta AK, Gupta M (2005) Biomaterials 26:3995